Accounting for stochasticity in demographic compensation along the elevational range of an alpine plant

Marco Andrello[1]*, Pierre de Villemereuil[2], Marta Carboni[3], Delphine Busson[4], Marie-Josée Fortin[5], Oscar E. Gaggiotti[6] and Irène Till-Bottraud[7]

[1] MARBEC, Univ Montpellier, CNRS, IFREMER, IRD, Sète, France. Email: marco.andrello@gmail.com. Tel: +33 4 99 57 32 16. ***Corresponding author**

[2] EPHE PSL University, Institut de Systématique, Evolution et Biodiversité, UMR 7205, CNRS, MNHN, Sorbonne Université, Paris, France. Email: pierre.devillemereuil@ephe.psl.eu

[3] Dipartimento di Scienze, Università Degli Studi di Roma Tre, viale Marconi 446, 00146 Roma, Italy. Email: marta.carboni@gmx.net

[4] Laboratoire d'Ecologie Alpine (LECA), Université Grenoble Alpes, F-38000 Grenoble, France; CNRS, LECA, F-38000 Grenoble, France. Email: delphine_busson@yahoo.fr

[5] Department of Ecology and Evolutionary Biology, University of Toronto, Toronto, M5S 3B2, Canada. Email: mariejosee.fortin@utoronto.ca

[6] Scottish Oceans Institute, University of St Andrews, Fife, KY16 8LB, United Kingdom. Email: oeg@st-andrews.ac.uk

[7] Université Clermont Auvergne, CNRS, GEOLAB, F-63000 Clermont-Ferrand, France. Email: irene.till@uca.fr

Running title: Stochastic demographic compensation

Keywords: *Arabis alpina;* Brassicaceae; elasticity; elevation; population dynamics; stochasticity.

Article type: Letter

Word count: 144 (abstract), 4893 (main text)

Number of references: 60

Number of figures: 4

Number of tables: 2

Number of text boxes: 0

AUTHORSHIP

MA, ITB and OEG planned the study. MA, PDV and ITB carried out field work. MA, PDV, DB and MC analysed the environmental data. MA analysed the vital rates data with help from MJF. MA constructed and analysed the population dynamics model and led the writing. All authors contributed to the writing.

DATA ACCESSIBILITY

The data and R code used in this study are openly available in GitHub at https://github.com/MarcoAndrello/Stoch_Demogr_Comp_Arabis

ABSTRACT

Demographic compensation arises when vital rates change in opposite directions across populations, buffering the variation in population growth rates, and is a mechanism often invoked to explain the stability of species geographic ranges. However, studies on demographic compensation have disregarded the effects of temporal variation in vital rates and their temporal correlations, despite theoretical evidence that stochastic dynamics can affect population persistence in temporally varying environments. We carried out a seven-year-long demographic study on the perennial plant *Arabis alpina* across six populations encompassing most of its elevational range. We discovered demographic compensation in the form of negative correlations between the means of plant vital rates, but also between their temporal coefficients of variation, correlations and elasticities. Even if their contribution to demographic compensation was small, this highlights a previously overlooked, but potentially important, role of stochastic processes in stabilizing population dynamics at range margins.

INTRODUCTION

One of the processes shaping population performance across species ranges is demographic compensation between different vital rates, such as recruitment, survival, growth and reproduction (Doak & Morris 2010; Villellas *et al.* 2015). Demographic compensation arises when different vital rates change in opposite directions across populations in response to environmental gradients, and has been proposed as a mechanism increasing the range of environments over which a species can occur and to explain the apparent stability of species range margins despite strong temporal environmental changes (Doak & Morris 2010; Sheth & Angert 2018). So far, the paradigm of demographic compensation has considered spatial differences in vital rates averaged over years, while disregarding the role of spatial differences in temporal variation of vital rates (Villellas *et al.* 2015). However, because temporal variation in vital rates can be higher in some parts of a species geographical range (for example, at range margins; Angert 2009; Pironon *et al.* 2017), population growth rates might vary across species ranges not only because of spatial variation in mean vital rates, but also in their temporal variability.

Population dynamics in temporally varying environments have received much attention in ecology and conservation (Tuljapurkar 1990; Lande *et al.* 2003). Theory predicts that temporal variability should decrease population growth rates in both structured and unstructured populations (Lewontin & Cohen 1969; Tuljapurkar 1990) and empirical studies support these predictions (Morris *et al.* 2008). In addition, positive temporal covariations between vital rates can potentially amplify the effects of environmental stochasticity on population dynamics, while negative temporal covariation can buffer it (Doak *et al.* 2005; Jongejans *et al.* 2010; Compagnoni *et al.* 2016). For example, positive covariances between reproduction and survival rates tend to magnify the effect of variability and lead to lower population growth rates than in the case of zero or negative covariances (Jongejans *et al.* 2010). Finally, the elasticities of population growth rates, which measure the change in population growth rate caused by a

change in demographic parameters, determine the ultimate effects of temporal variation and vital rate correlations on the population growth rate (Caswell 2001; Tuljapurkar *et al.* 2003). The interplay of these factors is perhaps best summarized by writing the stochastic population growth rate $\log\lambda_s$ using the small-noise approximation, as a function of the intrinsic growth rate $\log\lambda_d$ (calculated using the temporal means of vital rates) minus a product containing temporal coefficients of variation of vital rates (CV_k and CV_l), correlations between vital rates (ρ_{kl}) and vital rate elasticities (e_k and e_l) (Tuljapurkar 1990):

$$log\lambda_s \approx log\lambda_d - \frac{1}{2}\sum_{k,l} CV_k CV_l \rho_{k,l} e_k e_l \qquad \text{(eq. 1)}$$

Thus, a full picture of how population dynamics change across populations requires quantifying the differences in how mean vital rates, their temporal variation, their correlations and the elasticities change between populations. Such differences between populations can ultimately determine processes of demographic compensation and can thus inform on the stability and dynamics of species ranges (Doak & Morris 2010; Villellas *et al.* 2013).

Elevational ranges offer a unique opportunity to study range-wide variation in vital rates and population dynamics at a tractable spatial scale. For plants, elevational ranges have been associated with large differences in life-histories (Laiolo & Obeso 2017). Species living at lower elevations have often larger sizes, higher mortality rates, shorter lifespans and higher fecundities, while species living at higher elevations have smaller sizes, lower mortality rates, longer life spans and reduced flowering rates (Nobis & Schweingruber 2013; Laiolo & Obeso 2017). These life-history patterns have been related to predictions from the r-K selection theory (Pianka 1970), the metabolic theory of ecology (Brown *et al.* 2004) and the acquisitive and stress-tolerant strategies of functional ecology (Read *et al.* 2014). While many studies have uncovered elevational patterns in plant life-histories across species, studies on population dynamics are less common, and patterns of variation in plant population growth rates along elevational gradients are less clear. Indeed, the few studies focusing on dynamics of herbaceous plant

95 populations on elevational gradients report increasing (Miller *et al.* 2009; Giménez-Benavides *et al.*
96 2011), decreasing (Kim & Donohue 2011; Pena-Gomez & Bustamante 2012) and stable (García-Camacho
97 *et al.* 2012) patterns of population growth rates with elevation.

98 Here, we aimed at testing whether spatial patterns in temporal variation, temporal correlations and
99 elasticities could be involved in demographic compensation beyond the spatial variation of average vital
100 rates, thereby contributing to the stabilization of species elevational ranges. To this end, we carried out a
101 population dynamics study on *Arabis alpina* (Brassicaceae), a broadly distributed arctic-alpine perennial
102 herb, across most of its elevational range in the European Alps. Specifically, our goals were twofold. First,
103 we aimed at quantifying the spatial variation of four different descriptors of stochastic population
104 dynamics (means, coefficients of variation, correlations and elasticities of plant vital rates) across an
105 elevational gradient. Second, we aimed at quantifying the contributions of each of the four descriptors
106 to the stochastic population growth rate and test for demographic compensation between different
107 descriptors.

MATERIALS AND METHODS

Model species

Arabis alpina (L., Brassicaceae) is emerging as a new model organism in plant ecology and evolutionary biology (e.g. Wang *et al.* 2009; de Villemereuil *et al.* 2018) due to its perennial life-cycle and wide elevational distribution. It occurs primarily in the subalpine and alpine belts, predominantly in open, unstable, moist sites with low vegetation cover such as glacier forelands, scree slopes, rock ledges, footpaths and small streams, often in association with calcareous soil (Lauber *et al.* 2018). Seedlings germinate and establish throughout the growing season, plants flower for a few weeks and produce fruits (siliques), and flowering stems eventually wilt and die (Wang *et al.* 2009). Seeds can persist in the soil and form a permanent seed bank (Diemer & Prock 1993; Philipp *et al.* 2018).

Data collection

This study was conducted in six sites spanning most of the elevational range of *A. alpina* in the European Alps using permanent plots (**Table 1, Figure S1**), which were visited once a year after flowering between 2008 and 2014 to record the number of stems and siliques of each individual (See **Appendix S1.1** in **Supporting Information**). *In-situ* germination tests were not successful, so germination rates could not be estimated locally and seed bank dynamics was disregarded in the matrix population model, but we conducted a sensitivity analysis to assess the effects of uncertainty in seed germination on the results (Nguyen *et al.* 2019; **Appendix S1.5, S2.2**).

Microclimatic conditions, soil chemistry and species composition of the vegetation were measured in each plot to model plant vital rates in function of environmental conditions. Temperature data loggers (iButton® Hygrochron, Maxim Integrated™) provided estimates of summer daily mean temperature (T_{mean}) and daily temperature range (T_{range}; **Table 1**). Missing records (due to malfunctioning of the data-loggers) were imputed using data from nearby weather stations, resulting in ten resampled datasets

(**Appendix S1.2**). Soil acidity (pH), total soil carbon and nitrogen content were determined following standard methods (Schinner *et al.* 1996). Abundance-dominance (Braun-Blanquet) lists of plant species were used to calculate abundance weighted means for vegetative height and specific leaf area (SLA), using values from the ANDROSACE (Thuiller *et al.* 2014) and the TRY (Kattge *et al.* 2011) databases. After performing a principal component analysis on the three soil variables and the two vegetation variables (**Appendix 2.1, Figure S3, S4**), we retained the first two axes to predict plant vital rates: $SoilVeg_1$ (explaining 52% of the variance), positively related to acidic soils with high C and N content, and $SoilVeg_2$ (explaining 29% of the variance), summarizing variation from slow-growing short vegetation to fast-growing tall vegetation.

Analysis

We used a five-step approach to test how four *descriptors* (μ: means; *CV*: coefficients of variation; *E*: elasticities; ρ: temporal correlations) of seven *life-cycle components* (S: survival; G^-: retrogressive growth; $G^=$: stasis; G^+: progressive growth; F_0: reproduction; F_1: fecundity; F_2: recruit size) contribute to demographic compensation across the elevational range of *A. alpina*. First, we constructed matrix population models for each site and year using statistical models predicting plant vital rates from environmental variables (Step 1). Second, we used the matrix models to calculate the seven life-cycle components, stochastic population growth rate $\log\lambda_s$ and elasticities of $\log\lambda_s$ (Step 2). Third, we tested for significant relationships between elevation and population dynamics variables (Step 3). Fourth, we performed a stochastic life-table response experiment (SLTRE) in order to decompose the differences in $\log\lambda_s$ between sites into contributions C_l^k of each life-cycle component *l* and each descriptor *k* (Step 4). Finally, we assessed demographic compensation by testing for negative and positive correlations between the SLTRE contributions C_l^k (Step 5).

153 *Step 1. Prediction of plant vital rates*

154 The plant vital rates used to construct the matrix population models were survival (whether the plant
155 survives to t + 1 or not), size (the size of the plant at time t + 1, conditional on survival), reproduction
156 (whether the plant bears siliques or not at time t), reproductive output (the number of siliques of the
157 plant at time t, conditional on reproduction) and recruit size. Plant vital rates were predicted using
158 generalized linear mixed models (GLMMs; Zuur *et al.* 2009) as a function of plant size at time t (except
159 for recruit size that, by definition, did not exist at time t), T_{mean}, T_{range}, $SoilVeg_1$ and $SoilVeg_2$ treated as
160 fixed effects; plant size at time t and T_{mean} were also included as quadratic terms. Site, year nested within
161 site and plot nested within site were included as random effects on the intercept and the slopes when
162 significant. The error structure of the models was Gaussian (for $\log_{10}$-transformed reproductive output),
163 Bernoulli (for survival and reproduction), or negative binomial (for growth and recruit size). We
164 accounted for uncertainty in the data using a total 2000 bootstrap samples over the ten imputed climatic
165 datasets. For each bootstrap sample, we fitted the 2^7=128 models corresponding to the combinations of
166 the predictors, sampled one of them according to its Akaike weight (Burnham & Anderson 2002),
167 obtained site- and year-specific predictions of vital rates (by setting predictors to their mean values over
168 the plots of each site and year) and constructed matrix models to perform all the subsequent population
169 dynamics analyses. Means and 95% confidence intervals for the reported results were calculated from
170 the 2000 predicted values using the percentile method. All analyses were run in R 3.6.0 with packages
171 *lme4* 1.1-21 and *MuMIn* 1.43.6 (Bartoń 2009; Bates et al. 2015; **Appendix S1.3**).

172 *Step 2. Population dynamics analyses*

173 We defined a matrix population model (Caswell 2001) with 50 size classes of one-stem each, which
174 covered the range of variation in plant sizes observed in the field. The projection matrix **A** was the sum
175 of the transition matrix **P** = [p_{ij}] and the fecundity matrix **F** = [f_{ij}], which were constructed using the
176 predicted vital rates obtained in Step 1:

177 $p_{ij} = s_j g_{ij}$

178 $f_{ij} = \varepsilon F_{0,j} F_{1,j} F_{2,i}$ (eq. 2)

179 where *j* is plant size in year *t*; *i* is plant size in year *t+1*; s_j (survival) g_{ij} (growth), $F_{0,j}$ (reproduction), $F_{1,j}$
180 (reproductive output) and $F_{2,i}$ (recruit size) are the predicted vital rates. ε = 0.02 is a seedling
181 establishment coefficient converting the number of fruits in one year to the number of seedling in the
182 following year, and was set equal to the median value of the ratio of the observed number of seedlings
183 to the number of fruits in the previous year over all plots and sites.

184 Life-cycle components for each site and year were calculated as averages of the predicted vital rates over
185 size classes weighted by the stable stage distribution vector (Salguero-Gómez *et al.* 2016). Specifically, S,
186 F_0 and F_1 were calculated as weighted averages of the s_j's, $F_{0,j}$'s and $F_{1,j}$'s (eq. 2), respectively. G^-
187 represents transitions from larger to smaller size classes and was calculated as the weighted average of
188 all the g_{ij}'s for which $i < j$. Similarly, $G^=$ (representing individuals not changing in size) and G^+ (representing
189 transitions to larger size classes) were calculated as weighted averages of all the g_{ij}'s for which $i = j$ and i
190 $> j$, respectively. F_2 was calculated as the mean recruit size distribution $F_{2,i}$.

191 For each site, we calculated the temporal means and coefficients of variation of each life-cycle
192 component and temporal correlations between pairs of life-cycle components (Pearson's correlation)
193 over years. The stochastic population growth rate $\log\lambda_s$ was calculated via the simulation method by
194 randomly sampling one of the year-specific matrix at each iteration (Caswell 2001, p. 396). We then
195 calculated the elasticities of $\log\lambda_s$ to changes in the mean and standard deviation of the stage-specific
196 vital rates (Tuljapurkar *et al.* 2003). We obtained the elasticities to the mean and standard deviation of
197 life-cycle components by summing the elasticities of the respective vital rates (Franco & Silvertown 2004;
198 **Appendix S1.4**).

Step 3. Elevational patterns

We used linear regressions to test for significant relationships between elevation and population dynamics variables: mean life-cycle components, coefficients of variation of life-cycle components, temporal correlations between life-cycle components, logλ_s and elasticities.

Step 4. Stochastic life-table response experiment (SLTRE)

We calculated the differences in logλ_s ($\Delta \log \lambda_s^{(m)}$) between each site *m* and a common reference site defined by the means of vital rates over sites. The $\Delta \log \lambda_s^{(m)}$ were decomposed into the contributions $C_{x_i,x_j}^{k,(m)}$ of differences of each descriptor *k* (mean μ; coefficient of variation *CV*; temporal correlations ρ; elasticities *e*) of stage-specific vital rates x_i (survival s_j, growth g_{ij}, reproduction $F_{0,j}$, reproductive output $F_{1,j}$ and recruit size $F_{2,i}$) according to the SLTRE of Davison *et al.* (2013; **Appendix S1.6**):

$$\Delta \log \lambda_s^{(m)} \approx \sum_i C_{x_i}^{\mu,(m)} + \sum_{i,j} C_{x_i,x_j}^{CV,(m)} + \sum_{i,j} C_{x_i,x_j}^{\rho,(m)} + \sum_{i,j} C_{x_i,x_j}^{e,(m)} \quad \text{(eq. 3)}$$

From this decomposition, we derived the *net contributions* C_l^k of each life-cycle component *l* and each descriptor *k* by summing the $C_{x_i,x_j}^{k,(m)}$ according to the definition of life-cycle components given above. The *total effect* C_l of each life-cycle component was calculated by summing the absolute values of its contributions over the four descriptors, $C_l = \sum_k |C_l^k|$. Similarly, the *total effect* C^k of each descriptor was calculated by summing the absolute values of its contributions over life-cycle components, $C^k = \sum_l |C_l^k|$. Finally, we used linear regressions to test for significant relationships between elevation and the net contributions C_l^k.

Step 5. Demographic compensation

To test for demographic compensation and its effectiveness in reducing the spatial variation in population growth rates, we extended the approach of Villellas *et al.* (2015) to all descriptors of life-cycle components. We tested for demographic compensation by testing for negative and positive Spearman

correlations between the net contributions C_i^k. The occurrence of a significantly higher number of significant negative correlations (or a significantly lower number of significant positive correlations) than expected by chance is indicative of demographic compensation and was tested by permuting 1000 times the C_i^k over sites. This permutation test assesses only the occurrence of demographic compensation but not its effectiveness in reducing the variance in $\log\lambda_s$ among sites, $\sigma^2_{\log\lambda_s}$. We then performed additional randomization tests where we calculated $\sigma^2_{\log\lambda_s}$ following the permutation of each net contribution C_i^k at a time (thus 28 parameters). Higher values of $\sigma^2_{\log\lambda_s}$ in the randomization indicated that the focal parameter reduced $\sigma^2_{\log\lambda_s}$ through its negative correlations; conversely, lower values for $\sigma^2_{\log\lambda_s}$ indicated that the focal parameter increased $\sigma^2_{\log\lambda_s}$ through its positive correlations. Finally, we ran a randomization test where we permuted only those C_i^k that reduced $\sigma^2_{\log\lambda_s}$: this randomization procedure eliminates as much as possible the negative correlations while preserving the important positive correlations and indicates the overall effectiveness of demographic compensation (Villellas *et al.* 2015).

RESULTS

Step 1. Prediction of plant vital rates

Plant size had significant effects on all vital rates (**Table 2**). Size and reproductive output were positively affected by *SoilVeg*$_2$, which was itself positively related to vegetative height and SLA of the surrounding vegetation (**Appendix S2.1**). Survival was positively affected by mean temperature squared (T^2_{mean}), while recruit size was negatively affected by temperature range (T_{range}). However, the models for survival and recruit size had remarkably low explanatory power (marginal R^2 = 0.07 and 0.04, respectively). All vital rates showed considerable spatial and temporal variation that was unexplained by our environmental variables (conditional R^2 larger than marginal R^2).

Step 2. Population dynamics analyses

On average, survival probability was S = 0.5 (except in GAL where S = 0.75), progressive growth (G^+) was larger than retrogressive growth (G^-) and stasis ($G^=$), reproduction was F_0 = 0.5, reproductive output was F_1 = 12 siliques and recruit size was F_2 = 1.5 stems (**Figure 1 and S5**). Coefficients of variations (CV) were mostly comprised between 0.1 and 0.6 across all life-cycle components. Over all sites and pairs of life-cycle components, we observed 21 (17%) significant negative temporal correlations and 21 (17%) significant positive temporal correlations (**Figure S6**).

The stochastic population growth rate $\log\lambda_s$ was negative in all sites (**Table 1**). One site (GAL) had higher $\log\lambda_s$ than the other sites. The largest elasticities of $\log\lambda_s$ to the temporal means of life-cycle components were associated with S, while the elasticities to G^+ were the second-largest (**Figure 1**). The elasticities of $\log\lambda_s$ to the standard deviation of life-cycle components were largest and negative for S, intermediate for G^+ and F_1, and smallest for G^-, $G^=$, F_0 and F_2.

Step 3. Elevational patterns

Mean survival (S), retrogressive growth (G^-) and stasis ($G^=$) increased significantly with elevation (**Figure 1**), while mean progressive growth (G^+), reproductive output (F_1) and recruit size (F_2) decreased significantly with elevation. The CV of S, G^- and $G^=$ decreased significantly with elevation.

While the elasticities to mean S did not change with elevation, the elasticities to mean G^+ significantly decreased with elevation. The elasticities to the means of the other life-cycle components were much smaller and showed significant positive (G^- and $G^=$) or negative (F_0, F_1 and F_2) relationships with elevation. The elasticities to the standard deviation of life-cycle components did not change significantly with elevation, nor did the temporal correlations between life-cycle components.

The stochastic growth rate $\log\lambda_s$ did not change significantly with elevation (**Figure S7**).

Step 4. Stochastic life-table response experiment (SLTRE)

The SLTRE showed that all four descriptors of life-cycle components (means, coefficients of variation, temporal correlations and elasticities) contributed to differences in $\log\lambda_s$ between sites (**Figure 2**). Means had the largest total effects in all sites, but the other descriptors were not negligible and could account for up to 50% of the difference in the stochastic growth rate (**Figure 2a**): the largest effects were due to coefficients of variation, while elasticities and correlations had smaller effects. When looking at the total effects of each life-cycle component (**Figure 2b**), the largest ones were due to survival (S) and progressive growth (G^+), while the other life-cycle components had smaller effects.

The net contributions of means and coefficients of variation of S (C_S^{μ} and C_S^{CV}) increased (became more positive) with elevation, while the net contributions of mean G^+ ($C_{G^+}^{\mu}$) decreased (became more negative) with elevation (**Figure S8**).

Step 5. Demographic compensation

There were 18 significant positive correlations and 22 significant negative correlations between the net contributions of life-cycle components across sites. This constitutes substantial evidence for the existence of demographic compensation according to the criterion proposed by Villellas *et al.* (2015), since the number of negative correlations was much higher than expected by chance (permutation test, **Figure 3**).

The negative correlations involved all four descriptors of population dynamics. While the correlations linking G^-, $G^=$ and G^+ together are trivial as they emerge from the same vital process (growth), the other correlations are ecologically meaningful (**Figure S9**). Among these, there were significant negative correlations involving mean life-cycle components (S, G^+, F_1 and F_2), their coefficients of variation (S), temporal correlations (S, G^- and $G^=$) and elasticities (G^- and G^+). Significant negative correlations linked together the same descriptor of different life-cycle component (e.g. mean S and mean F_1), different descriptors of the same life-cycle component (e.g. mean G^+ and its elasticity) and different descriptors of different life-cycle components (the CV of S and the mean of G^+, F_1 and F_2).

The parameters contributing the most to demographic compensation were mean S, mean G^+ and mean F_1, as their permutation generally increased the variance of $\log\lambda_s$ between sites, $\sigma^2_{\log\lambda_s}$ (**Figure 4a-d**). Conversely, the permutation of the CV of S led to smaller $\sigma^2_{\log\lambda_s}$, indicating that this parameter increases the variance in $\log\lambda_s$ relative to what would be expected by chance; this was the result of the numerous positive correlations involving the CV of S (**Figure 3**). The other parameters did not change $\sigma^2_{\log\lambda_s}$ considerably. Randomizing only the parameters that reduced the variance in $\log\lambda_s$ between sites indicated that the observed $\sigma^2_{\log\lambda_s}$ was 59% of the median $\sigma^2_{\log\lambda_s}$ expected under the hypothesis of minimal negative correlations, but not significantly smaller (p = 0.17; **Figure 4e**).

DISCUSSION

In this work, we studied variation in population dynamics of *A. alpina* across most of its elevational range in the European Alps (2000m). Contrary to the expectation that peripheral populations have lower demographic performance than central populations (Pironon *et al.* 2017), *A. alpina* showed surprisingly little variation in population growth rates $\log\lambda_s$ across its full elevational range. Conversely, most life-cycle components significantly varied with elevation. We showed that this pattern could be partly explained by demographic compensation, *i.e.* negative correlations between the contributions of different life-cycle components to spatial differences in $\log\lambda_s$. In particular, compensatory effects across the elevational range did not arise only through opposite spatial patterns in mean vital rates, but also in their temporal variation, elasticities and temporal correlations. This highlights a previously overlooked, but potentially important, role of stochastic processes in offsetting mean changes in vital rates and stabilizing population dynamics at range margins. We now discuss the origin, significance and generalities of the patterns of demographic compensation observed in this study.

The origin of negative correlations between the different descriptors of life-cycle components should be searched in their patterns of variation along the elevational gradient (**Figure 1**). First, mean vital rates changed in opposite directions: survival (S) increased along the elevational gradient while reproductive output (F_1) decreased, resulting in a negative correlation between C_S^{μ} and $C_{F_1}^{e}$ (**Figure S9**). However, stochastic descriptors also contributed to demographic compensation along elevation. For example, the decrease in mean progressive growth (G^+), by itself, should have resulted in lower population growth rates $\log\lambda_s$ at higher elevations. However, the elasticity to mean G^+ also decreased with elevation and counterbalanced the negative effects of lower G^+, because smaller elasticities dampen the effects of changes in life-cycle components on $\log\lambda_s$. The CV of survival also decreased with elevation, further offsetting the negative effects of lower G^+, since smaller CV have positive effects on $\log\lambda_s$. The resulting

negative correlations between the net contributions of these parameters to logλ_s (namely, between $C^{\mu}_{G^+}$ and $C^{e}_{G^+}$ and between $C^{\mu}_{G^+}$ and C^{CV}_{S}) partly explain why population growth rates did not change with elevation despite marked elevational gradients in life-cycle components. Overall, the observed patterns are in agreement with the known higher occurrences of smaller and longer lived species and individuals at higher elevations (Nobis & Schweingruber 2013; Laiolo & Obeso 2017) and higher variability of survival at lower elevations (Angert 2009).

Such elevational patterns could be due to opposite responses of vital rates to common environmental drivers (Knops *et al.* 2007). The main environmental driver of variation in growth and reproductive output was $SoilVeg_2$, which summarizes variation in specific leaf area (SLA) and vegetative height (**Appendix S2.1**)**,** meaning that *A. alpina* tends to grow larger and produce more fruits when the surrounding vegetation is composed of tall plants with large SLA. This relationship could indicate a response to high competitive pressure or a common effect of temperature, because SLA and vegetative height in plants tend to increase with temperature and decrease with elevation (Moles *et al.* 2014; Read *et al.* 2014; Rosbakh *et al.* 2015). In contrast, the environmental drivers of survival are not easy to identify, because the statistical model linking plant survival probability to environmental variables had very low explanatory power. These results seem corroborated by a common garden experiment using the same six populations as this study, which found that temperature was significantly associated with total fruit length (a measure of reproductive output) but not with survival (de Villemereuil et al. 2018). Elevational patterns in survival, growth and reproductive output could also be driven by other environmental factors not considered in our analysis, such as soil phosphorus content, diversity of root microbiota or herbivore damage, all of which affect various traits of *A. alpina* across its range (Almario et al. 2017; Buckley et al. 2019). Negative correlations between life-cycle components could also be due to energetic trade-offs and structural constraints (Williams *et al.* 2015). In *A. alpina*, higher rates of flowering are associated with reduction of plant survival, because all stems wilt and die after setting

seeds, to the point that mutants for perpetual flowering show an annual life-cycle (Wang *et al.* 2009). Slower rates of stem production and/or lower rates of flowering could thus increase the longevity of the entire plant, resulting in negative correlations between growth, reproduction and survival.

Spatial patterns in elasticity are not very documented, but increasing elasticities to survival with elevation could result from their positive correlation with longevity (Silvertown *et al.* 1993; Franco & Silvertown 2004) and from the positive correlation between longevity and elevation (Nobis & Schweingruber 2013). In contrast, decreasing elasticities to fecundity and growth with elevation, as found in our study, could be expected given that these elasticities correlate with SLA (Adler *et al.* 2014) and SLA is known to decrease with elevation (Read *et al.* 2014). However, within-species patterns of elasticities are also influenced by the level of environmental disturbance (Oostermeijer *et al.* 1996; Silvertown *et al.* 1996), which may not show consistent variation with elevation.

The correlations between life-cycle components involved all descriptors of population dynamics but their effectiveness for reducing the variance in $\log\lambda_s$ ($\sigma^2_{\log\lambda_s}$) was higher in the case of mean life-cycle components. The effectiveness of a single descriptor for reducing $\sigma^2_{\log\lambda_s}$ through demographic compensation depends on the strength and number of its negative correlations relative to its positive correlations (**Figure 3**) and its contribution to the differences in $\log\lambda_s$ between sites, $\Delta\log\lambda_s$ (**Figure 2**). Only parameters making large contributions change $\sigma^2_{\log\lambda_s}$ through their correlations, decreasing it when most of their correlations are strong and negative. Mean progressive growth was the most important parameter for demographic compensation by offsetting variation in survival. Mean survival and mean reproductive output were the second most important parameters, thanks to their large contributions to $\Delta\log\lambda_s$ and the negative correlation between them. Conversely, temporal correlations and elasticities showed many significant negative correlations but they were not as important for demographic compensation because the net contributions to $\Delta\log\lambda_s$ were small, in line with what is observed in other

368 plant species (Jongejans *et al.* 2010; Compagnoni *et al.* 2016; Davison *et al.* 2019). Finally, the CV of
369 survival made relatively large contributions to $\Delta\log\lambda_s$, but showed too many positive correlations that led
370 to an increase of $\sigma^2_{\log\lambda_s}$ rather than a reduction.

371 Although our results are comparable to findings over multiple species in the deterministic case (Villellas
372 *et al.* 2015), our study is the first assessing demographic compensation in a stochastic framework.
373 Assessing whether the results obtained here are representative of other species will require additional
374 studies quantifying both the contributions of all descriptors of population dynamics to $\Delta\log\lambda_s$ and their
375 pairwise correlations. The first exercise has been done by Davison *et al.* (2019) on a set of 62 species,
376 showing that more than one quarter of contributions to $\Delta\log\lambda_s$ can be attributed to the effect of
377 coefficients of variations, elasticities and temporal correlations. However, the importance of these
378 descriptors of population dynamics for demographic compensation remains unknown, as it depends
379 critically on the relative number and strength of negative *vs.* positive correlations in which they are
380 involved.

381 Even with demographic compensation, the stochastic population growth rate was negative in all sites,
382 indicating that populations are projected to decline in size and eventually go extinct locally. However, *A.*
383 *alpina* could persist thanks to germination from its persistent seed bank and immigration from other
384 sites (Hastings & Botsford 2006). Its frequent occurrence in unstable sites suggests that populations
385 could show an extinction-recolonization dynamics typical of metapopulations (Ouborg & Eriksson 2004).
386 The inclusion of a seed bank led to higher, sometimes positive population growth rates and confirmed
387 the existence of demographic compensation (**Appendix S2.2**). The effects of immigration are more
388 difficult to study in absence of estimates of seed dispersal rates, but the strong spatial genetic structure
389 of the populations (F_{ST} = 0.6, de Villemereuil *et al.* 2018) suggests that dispersal rates might be low. The
390 patterns of demographic compensation revealed here could thus be different in models integrating
391 empirical estimates of seed dormancy and germination rates and extinction-recolonization dynamics,

potentially unmasking greater importance for coefficients of variation, elasticities and temporal correlations.

So far, demographic compensation has been discussed mainly in terms of spatial variation in mean vital rates (Doak & Morris 2010; Villellas *et al.* 2015; Sheth & Angert 2018). Our study is the first to highlight that temporal variation, elasticities and temporal correlations can be involved in demographic compensation, even if their effect was smaller than that of means. Nonetheless, temporal variation in vital rates could become more important under future expected increasing frequencies of extreme climatic events (Meehl & Tebaldi 2004; Schär *et al.* 2004), such as summer heatwaves and drought, that can cause large temporal variation in vital rates (Smith 2011; Andrello *et al.* 2012). Assessing the importance of all descriptors of population dynamics for demographic compensation could thus provide a more complete understanding of the dynamics of elevational as well as geographical species ranges in a context of global change.

ACKNOWLEDGEMENTS

We thank Serge Aubert, Rolland Douzet and Bénédicte Poncet for helping us find the populations, Hannah Secher Frommel and Cindy Arnoldi for soil analyses, Anne Delestrade for providing the weather station data, three anonymous reviewers whose comments helped us improve the manuscript and all the people who helped us in the field (in particular Florian Alberto, Perrine Augrit, Anne-Lise Bartalucci, Justine Bisson, Jérémy Camazzola, Loïc Chalmandrier, Julie Chauvin, Lucas Hemery, Elsa Jullien, Aymeric Pilleux, Blaise Tymen and Stefan Willhoit). MA and PDV were funded by a PhD scholarship by the French Ministry of Research. This research was partially conducted at the Jardin Alpin du Lautaret, a member of the AnaEE network (Infrastructure for Analysis and Experimentation on Ecosystems), and has used plant trait values from the TRY initiative and data base (http:// www.try-db.org), which is hosted, developed and maintained by J. Kattge and G. Bonisch (Max Planck Institute for Biogeochemistry, Jena, Germany), and currently supported by DIVERSITAS/Future Earth and the German Centre for Integrative Biodiversity Research (iDiv) Halle-Jena-Leipzig.

LITERATURE CITED

Adler, P.B., Salguero-Gomez, R., Compagnoni, A., Hsu, J.S., Ray-Mukherjee, J., Mbeau-Ache, C., *et al.* (2014). Functional traits explain variation in plant life history strategies. *Proceedings of the National Academy of Sciences*, 111, 740–745.

Almario, J., Jeena, G., Wunder, J., Langen, G., Zuccaro, A., Coupland, G., *et al.* (2017). Root-associated fungal microbiota of nonmycorrhizal Arabis alpina and its contribution to plant phosphorus nutrition. *PNAS*, 114, E9403–E9412.

Andrello, M., Bizoux, J.-P., Barbet-Massin, M., Gaudeul, M., Nicolè, F. & Till-Bottraud, I. (2012). Effects of management regimes and extreme climatic events on plant population viability in *Eryngium alpinum*. *Biological Conservation*, 147, 99–106.

Angert, A.L. (2009). The niche, limits to species' distributions, and spatiotemporal variation in demography across the elevation ranges of two monkeyflowers. *Proceedings of the National Academy of Sciences*, 106, 19693–19698.

Bartoń, K. (2009). *MuMIn: multi-model inference*. R package. .

Bates, D., Maechler, M., Bolker, B. & Walker, S. (2015). Fitting Linear Mixed-Effects Models Using lme4. *Journal of Statistical Software*, 67, 1–48.

Brown, J.H., Gillooly, J.F., Allen, A.P., Savage, V.M. & West, G.B. (2004). Toward a metabolic theory of ecology. *Ecology*, 85, 1771–1789.

Buckley, J., Widmer, A., Mescher, M.C. & De Moraes, C.M. (2019). Variation in growth and defence traits among plant populations at different elevations: Implications for adaptation to climate change. *Journal of Ecology*, 107, 2478–2492.

Burnham, K.P. & Anderson, D.R. (2002). *Model Selection and Multimodel Inference: A Practical Information-Theoretic Approach*. 2nd edn. Springer-Verlag, New York.

Caswell, H. (2001). *Matrix population models. Construction, analysis and interpretation*. Sinauer, Massachussets.

Compagnoni, A., Bibian, A.J., Ochocki, B.M., Rogers, H.S., Schultz, E.L., Sneck, M.E., *et al.* (2016). The effect of demographic correlations on the stochastic population dynamics of perennial plants. *Ecological Monographs*, 86, 480–494.

Davison, R., Nicolè, F., Jacquemyn, H. & Tuljapurkar, S. (2013). Contributions of Covariance: Decomposing the components of stochastic population growth in Cypripedium calceolus. *Am Nat*, 181.

Davison, R., Stadman, M. & Jongejans, E. (2019). Stochastic effects contribute to population fitness differences. *Ecological Modelling*, 408, 108760.

Diemer, M. & Prock, S. (1993). Estimates of Alpine Seed Bank Size in Two Central European and One Scandinavian Subarctic Plant Communities. *Arctic and Alpine Research*, 25, 194.

Doak, D.F. & Morris, W.F. (2010). Demographic compensation and tipping points in climate-induced range shifts. *Nature*, 467, 959–962.

Doak, D.F., Morris, W.F., Pfister, C., Kendall, B.E. & Bruna, E.M. (2005). Correctly Estimating How Environmental Stochasticity Influences Fitness and Population Growth. *The American Naturalist*, 166, E14–E21.

Franco, M. & Silvertown, J. (2004). A comparative demography of plants based upon elasticities of vital rates. *Ecology*, 85, 531–538.

García-Camacho, R., Albert, M.J. & Escudero, A. (2012). Small-scale demographic compensation in a high-mountain endemic: the low edge stands still. *Plant Ecology & Diversity*, 5, 37–44.

Giménez-Benavides, L., Albert, M.J., Iriondo, J.M. & Escudero, A. (2011). Demographic processes of upward range contraction in a long-lived Mediterranean high mountain plant. *Ecography*, 34, 85–93.

Hastings, A. & Botsford, L.W. (2006). Persistence of spatial populations depends on returning home. *Proceedings of the National Academy of Sciences of the United States of America*, 103, 6067–6072.

Jongejans, E., Kroon, H.D., Tuljapurkar, S. & Shea, K. (2010). Plant populations track rather than buffer climate fluctuations. *Ecology Letters*, 13, 736–743.

Kattge, J., Díaz, S., Lavorel, S., Prentice, I.C., Leadley, P., Bönisch, G., *et al.* (2011). TRY – a global database of plant traits. *Global Change Biology*, 17, 2905–2935.

Kim, E. & Donohue, K. (2011). Demographic, developmental and life-history variation across altitude in Erysimum capitatum. *J. Ecol.*, 99, 1237–1249.

Knops, J.M.H., Koenig, W.D. & Carmen, W.J. (2007). Negative correlation does not imply a tradeoff between growth and reproduction in California oaks. *Proc Natl Acad Sci U S A*, 104, 16982–16985.

Laiolo, P. & Obeso, J.R. (2017). Life-History Responses to the Altitudinal Gradient. In: *High Mountain Conservation in a Changing World* (eds. Catalan, J., Ninot, J.M. & Aniz, M.M.). Springer International Publishing, Cham, pp. 253–283.

Lande, R., Engen, S. & Saether, B.-E. (2003). *Stochastic Population Dynamics in Ecology and Conservation*. Oxford University Press.

Lauber, K., Gerhart, W. & Gygax, A. (2018). *Flora Helvetica - Flore illustrée de Suisse*. Haupt Verlag.

Lewontin, R.C. & Cohen, D. (1969). On Population Growth in a Randomly Varying Environment. *Proceedings of the National Academy of Sciences of the United States of America*, 62, 1056–1060.

Meehl, G.A. & Tebaldi, C. (2004). More Intense, More Frequent, and Longer Lasting Heat Waves in the 21st Century. *Science*, 305, 994–997.

Miller, T.E.X., Louda, S.M., Rose, K.A. & Eckberg, J.O. (2009). Impacts of insect herbivory on cactus population dynamics: experimental demography across an environmental gradient. *Ecological Monographs*, 79, 155–172.

Moles, A.T., Perkins, S.E., Laffan, S.W., Flores-Moreno, H., Awasthy, M., Tindall, M.L., *et al.* (2014). Which is a better predictor of plant traits: temperature or precipitation? *Journal of Vegetation Science*, 25, 1167–1180.

Morris, W.F., Pfister, C.A., Tuljapurkar, S., Haridas, C.V., Boggs, C.L., Boyce, M.S., *et al.* (2008). Longevity Can Buffer Plant and Animal Populations Against Changing Climatic Variability. *Ecology*, 89, 19–25.

Nakagawa, S., Johnson, P.C.D. & Schielzeth, H. (2017). The coefficient of determination R2 and intra-class correlation coefficient from generalized linear mixed-effects models revisited and expanded. *Journal of The Royal Society Interface*, 14, 20170213.

Nguyen, V., Buckley, Y.M., Salguero-Gómez, R. & Wardle, G.M. (2019). Consequences of neglecting cryptic life stages from demographic models. *Ecological Modelling*, 408, 108723.

Nobis, M.P. & Schweingruber, F.H. (2013). Adult age of vascular plant species along an elevational land-use and climate gradient. *Ecography*, 36, 1076–1085.

Oostermeijer, J.G.B., Brugman, M.L., De Boer, E.R. & Nijs, H.C.M.D. (1996). Temporal and Spatial Variation in the Demography of Gentiana Pneumonanthe, a Rare Perennial Herb. *Journal of Ecology*, 84, 153–166.

Ouborg, N.J. & Eriksson, O. (2004). Toward a Metapopulation Concept for Plants. In: *Ecology, Genetics and Evolution of Metapopulations* (eds. Hanski, I. & Gaggiotti, O.E.). Academic Press, Burlington, pp. 447–469.

Pena-Gomez, F.T. & Bustamante, R.O. (2012). Life history variation and demography of the invasive plant Eschscholzia californica Cham. (Papaveraceae), in two altitudinal extremes, Central Chile. *Gayana Bot.*, 69, 113–122.

Philipp, M., Hansen, K., Monrad, D., Adsersen, H., Bruun, H.H. & Nordal, I. (2018). Hidden biodiversity in the Arctic – a study of soil seed banks at Disko Island, Qeqertarsuaq, West Greenland. *Nordic Journal of Botany*, 36, e01721.

Pianka, E.R. (1970). On r- and K-Selection. *The American Naturalist*, 104, 592–597.

Pironon, S., Papuga, G., Villellas, J., Angert, A.L., García, M.B. & Thompson, J.D. (2017). Geographic variation in genetic and demographic performance: new insights from an old biogeographical paradigm. *Biological Reviews*, 92, 1877–1909.

Poloczanska, E.S., Brown, C.J., Sydeman, W.J., Kiessling, W., Schoeman, D.S., Moore, P.J., *et al.* (2013). Global imprint of climate change on marine life. *Nature Climate Change*, 3, 919–925.

Read, Q.D., Moorhead, L.C., Swenson, N.G., Bailey, J.K. & Sanders, N.J. (2014). Convergent effects of elevation on functional leaf traits within and among species. *Functional Ecology*, 28, 37–45.

Rosbakh, S., Römermann, C. & Poschlod, P. (2015). Specific leaf area correlates with temperature: new evidence of trait variation at the population, species and community levels. *Alp Botany*, 125, 79–86.

Salguero-Gómez, R., Jones, O.R., Jongejans, E., Blomberg, S.P., Hodgson, D.J., Mbeau-Ache, C., *et al.* (2016). Fast–slow continuum and reproductive strategies structure plant life-history variation worldwide. *Proceedings of the National Academy of Sciences*, 113, 230–235.

Schär, C., Vidale, P.L., Lüthi, D., Frei, C., Häberli, C., Liniger, M.A., *et al.* (2004). The role of increasing temperature variability in European summer heatwaves. *Nature*, 427, 332–336.

Schinner, F., Öhlinger, R., Kandeler, E. & Margesin, R. (Eds.). (1996). *Methods in Soil Biology*. Springer-Verlag, Berlin Heidelberg.

Sheth, S.N. & Angert, A.L. (2018). Demographic compensation does not rescue populations at a trailing range edge. *PNAS*, 115, 2413–2418.

Silvertown, J., Franco, M. & Menges, E. (1996). Interpretation of Elasticity Matrices as an Aid to the Management of Plant Populations for Conservation. *Conservation Biology*, 10, 591–597.

Silvertown, J., Franco, M., Pisanty, I. & Mendoza, A. (1993). Comparative Plant Demography - Relative Importance of Life-Cycle Components to the Finite Rate of Increase in Woody and Herbaceous Perennials. *J. Ecol.*, 81, 465–476.

Smith, M.D. (2011). The ecological role of climate extremes: current understanding and future prospects: Ecological role of climate extremes. *Journal of Ecology*, 99, 651–655.

Thuiller, W., Guéguen, M., Georges, D., Bonet, R., Chalmandrier, L., Garraud, L., *et al.* (2014). Are different facets of plant diversity well protected against climate and land cover changes? A test study in the French Alps. *Ecography*, 37, 1254–1266.

Tuljapurkar, S. (1990). *Population Dynamics in Variable Environments*. Lecture Notes in Biomathematics. Springer Berlin Heidelberg, Berlin, Heidelberg.

Tuljapurkar, S., Horvitz, C.C. & Pascarella, J.B. (2003). The many growth rates and elasticities of populations in random environments. *The American Naturalist*, 162, 489–502.

Villellas, J., Doak, D.F., García, M.B. & Morris, W.F. (2015). Demographic compensation among populations: what is it, how does it arise and what are its implications? *Ecology Letters*, 18, 1139–1152.

Villellas, J., Morris, W.F. & García, M.B. (2013). Variation in stochastic demography between and within central and peripheral regions in a widespread short-lived herb. *Ecology*, 94, 1378–1388.

de Villemereuil, P., Mouterde, M., Gaggiotti, O.E. & Till-Bottraud, I. (2018). Patterns of phenotypic plasticity and local adaptation in the wide elevation range of the alpine plant Arabis alpina. *Journal of Ecology*, 106, 1952–1971.

Wang, R., Farrona, S., Vincent, C., Joecker, A., Schoof, H., Turck, F., *et al.* (2009). *PEP1* regulates perennial flowering in *Arabis alpina*. *Nature*, 459, 423–427.

Williams, J.L., Jacquemyn, H., Ochocki, B.M., Brys, R. & Miller, T.E.X. (2015). Life history evolution under climate change and its influence on the population dynamics of a long-lived plant. *Journal of Ecology*, 103, 798–808.

Zuur, A., Ieno, E.N., Walker, N., Saveliev, A.A. & Smith, G.M. (2009). *Mixed Effects Models and Extensions in Ecology with R*. Springer Science & Business Media.

SUPPORTING INFORMATION

Additional Supporting Information may be downloaded via the online version of this article at Wiley Online Library (www.ecologyletters.com).

Figure legends

Figure 1. Elevational patterns in life-cycle components and elasticities. Elevational patterns in mean life-cycle components, coefficients of variation (CV) of life-cycle components, elasticities to means (μ) and elasticities to standard deviation (σ) of life-cycle components. Life-cycle components are survival (S), retrogressive growth (G^-), stasis ($G^=$), progressive growth (G^+), reproduction (F_0), reproductive output (F_1) and recruit size (F_2). Dots are mean values and bars extend over 95% confidence intervals. The blue lines are fitted linear regressions between values and elevation, and the gray areas are 95% confidence intervals. Solid lines indicate significant regressions ($p < 0.05$). Confidence intervals and significance values were calculated by randomly sampling statistical models over 200 bootstrapped demographic datasets and 10 resampled imputed climatic datasets

Figure 2. Stochastic life-table response experiment (SLTRE). Total effects of each descriptor (a) and life-cycle component (b) to differences in stochastic population growth rates ($\log\lambda_s$) between the focal site and a reference site constructed by taking the mean of vital rates over all sites. (c) to (h), net contributions C_l^k of each descriptor *k* of each life-cycle component *l* to the difference in $\log\lambda_s$. Negative and positive contributions are plotted separately. Colours indicate the descriptor (μ, means; *E*, elasticities; *CV*, coefficients of variation; ρ, temporal correlations) or the life-cycle component (S, survival; G^-, retrogressive growth; $G^=$, stasis; G^+, progressive growth; F_0, reproduction; F_1, fecundity; F_2, recruit size).

Figure 3. Demographic compensation. Correlogram of Spearman's correlation coefficients between the net contributions of different descriptors of life-cycle components to differences in stochastic population growth rates ($\log\lambda_s$) between sites (SLTRE contributions). Negative correlations are in red, positive correlations are in blue. Boxes with thicker borders and an asterisk indicate significant correlations at $p <$ 0.05. The insets show the number of observed significant positive and negative correlations (vertical

591 dotted lines) compared to the distribution of the number expected by chance obtained through a
592 permutation test (histograms). See Figure 2 for definitions of descriptors and life-cycle components.

593 **Figure 4. Effectiveness of demographic compensation.** (a), variance of population growth rate $\log\lambda_s$
594 between sites, $\sigma^2_{\log\lambda_s}$, obtained by permuting each descriptor of each life-cycle component at a time.
595 Dots are mean values and bars extend over 95% confidence intervals over 1000 permutations. Values
596 higher than the observed $\sigma^2_{\log\lambda_s}$ (horizontal dashed line) indicate that the corresponding parameter
597 effectively reduces $\sigma^2_{\log\lambda_s}$ through demographic compensation. (b), observed $\sigma^2_{\log\lambda_s}$ (vertical dotted
598 lines) compared to the distribution of $\sigma^2_{\log\lambda_s}$ expected by chance obtained through permuting only the
599 parameters effectively reducing it (histograms). See Figure 2 for definitions of descriptors and life-cycle
600 components.

601

602 **FIGURE 1**

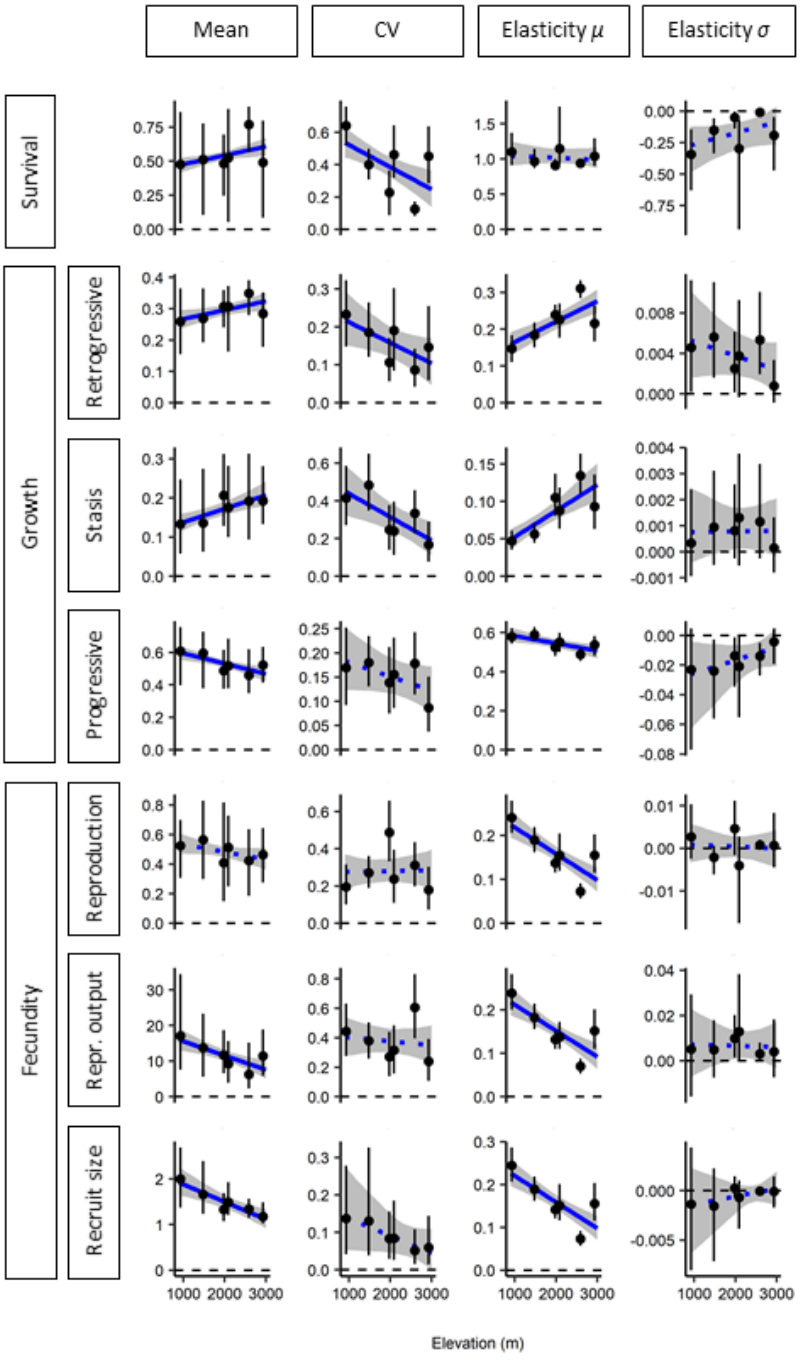

603

604 **FIGURE 2**

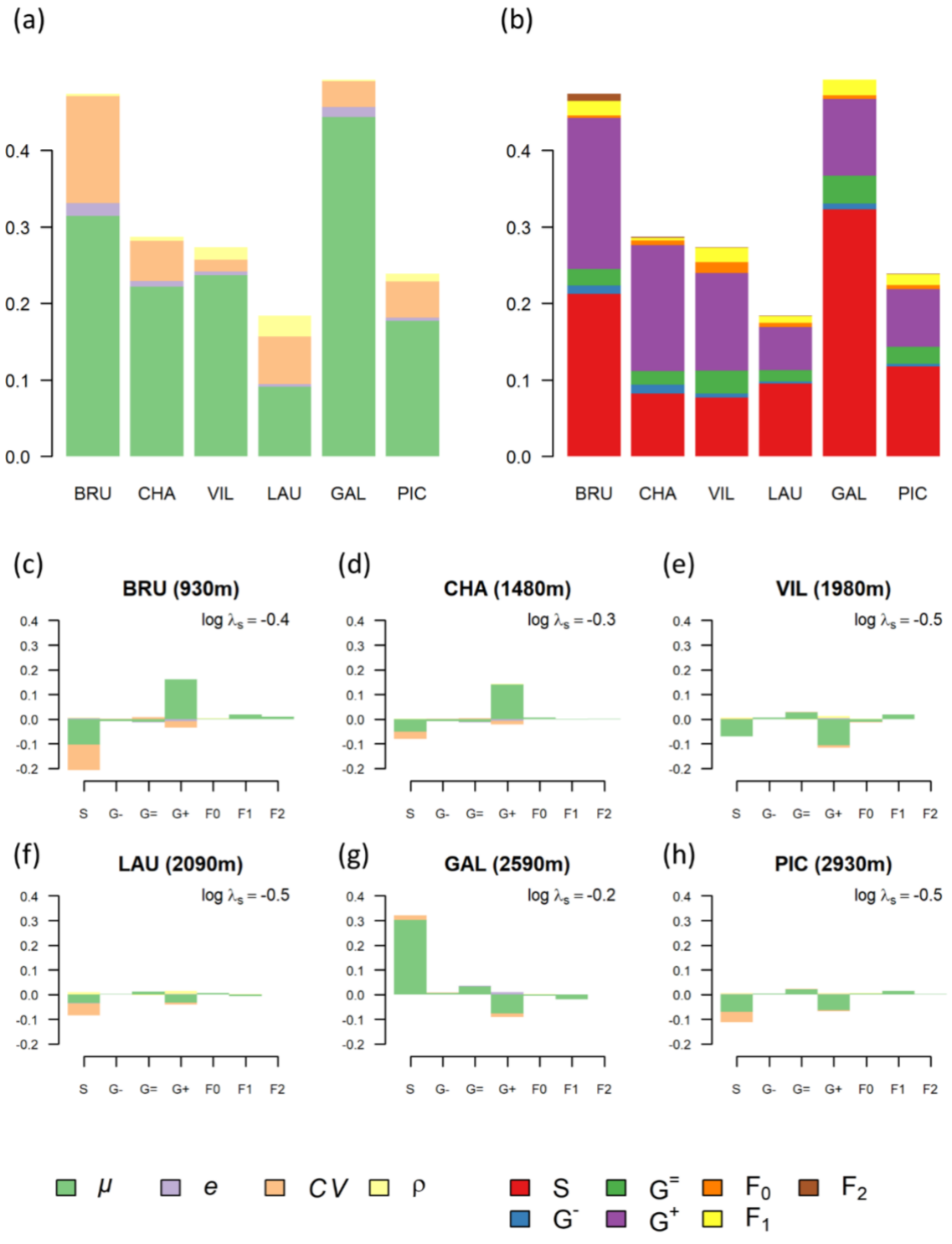

605

606 **FIGURE 3**

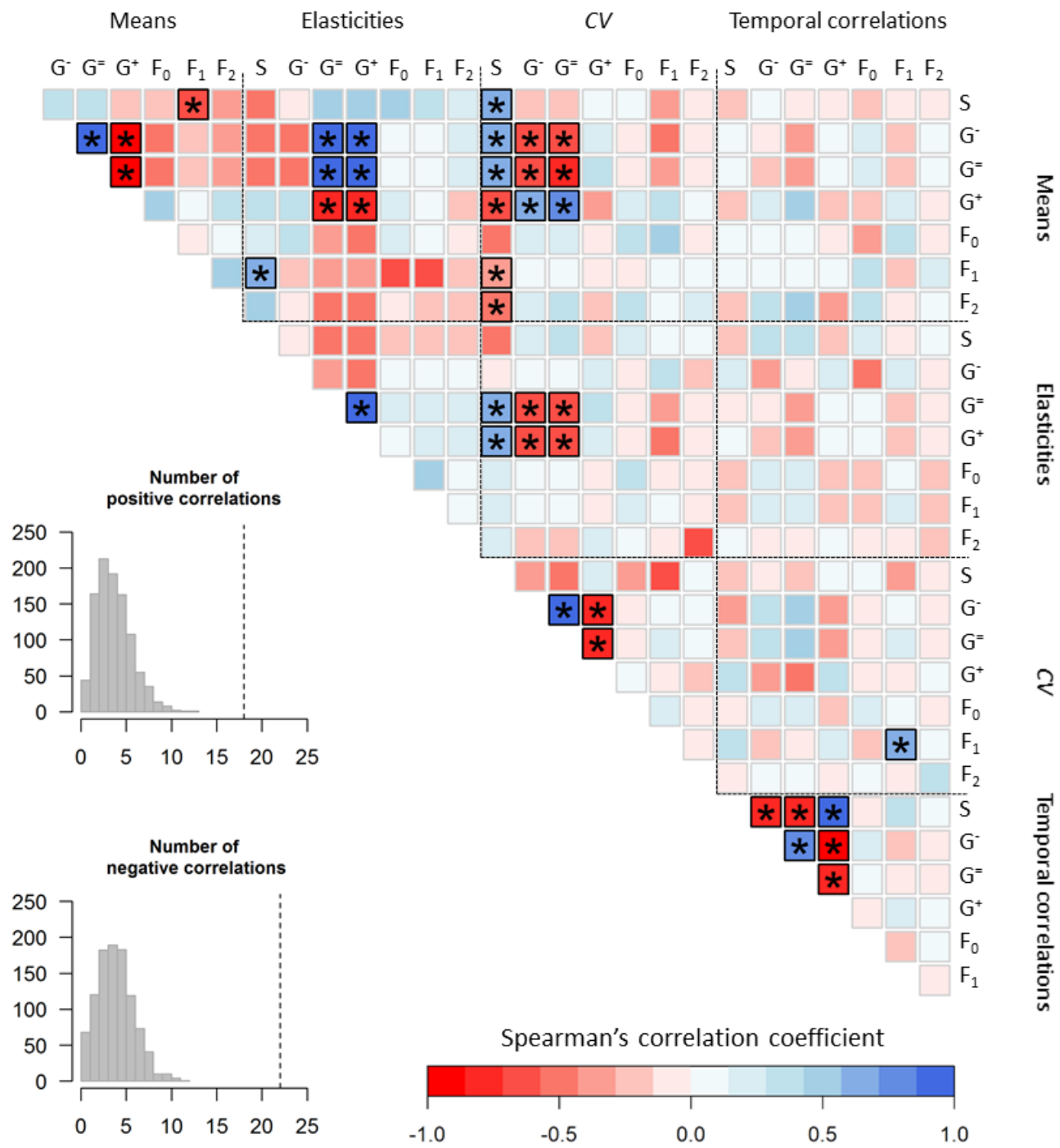

607

608

609 **FIGURE 4**

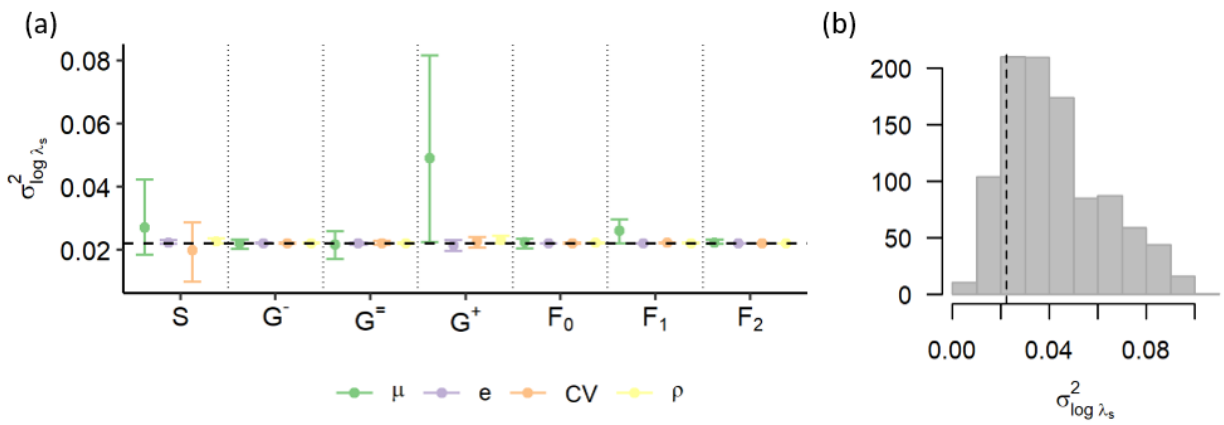

610

611

Table 1. Characteristics of the study sites.

Site	BRU	CHA	VIL	LAU	GAL	PIC
Longitude	5.61112	5.59267	5.57083	6.39034	6.40375	6.38426
Latitude	45.15065	45.07117	45.01809	45.02846	45.06049	45.06385
Elevation (m)	930	1480	1980	2090	2590	2930
Aspect	South	North	South	North	North	South
Habitat	Calcareous scree	Calcareous grassland, scree	Calcareous scree	Schists, torrent	Calcareous scree	Schistose scree
Initial *N*	46	145	104	90	110	50
Number of plots	2	3	3	3	3	4
T_{mean}	14.7 (12.8, 17.5)	15.7 (12.9, 18.2)	12.9 (9.3, 17.5)	10.4 (8.0, 12.1)	7.7 (5.3, 10.3)	9.1 (5.9, 12.1)
T_{range}	11 (6.0, 18.6)	16.9 (11.5, 21.9)	15.9 (9.7, 36.1)	6.3 (3.1, 9.6)	8.1 (5.8, 13.3)	16.3 (11.8, 23.2)
$\log\lambda_s$	-0.4 (-0.5, -0.2)	-0.3 (-0.5, -0.2)	-0.5 (-0.6, -0.4)	-0.5 (-0.8, -0.3)	-0.2 (-0.2, -0.1)	-0.5 (-0.8, -0.3)

N, number of individuals. Daily mean temperature (T_{mean}) and daily temperature range (T_{range}) were measured with *in-situ* data-loggers. Values are means and (minimum and maximum) over plots and years for the month of July. Means and 95% confidence interval for the stochastic population growth rate ($\log\lambda_s$) were calculated by randomly sampling the values calculated using matrix populations models constructed using predicted vital rates from 200 bootstrapped demographic datasets and 10 resampled imputed datasets. The *N* per site per year is shown in **Figure S2**.

Table 2. Statistical analysis of plant vital rates.

Predictor	Survival		Growth		Reproduction		Reproductive output		Recruit size	
	mean	95% CI	mean	95% CI	mean	95% CI	mean	95% CI	mean	95% CI
Fixed effects										
Intercept	**0.50**	**(0.31, 0.72)**	**1.35**	**(1.24, 1.44)**	**0.75**	**(0.35, 1.26)**	**1.05**	**(0.99, 1.10)**	**-0.76**	**(-1.11, -0.50)**
$SoilVeg_1$	-0.27	(-0.69, 0.19)	0.17	(-0.18, 0.35)	0.10	(-0.36, 0.77)	0.03	(-0.06, 0.15)	0.57	(-0.16, 1.07)
$SoilVeg_2$	-0.29	(-0.77, 0.05)	**0.17**	**(0.03, 0.38)**	0.14	(-0.26, 0.69)	**0.10**	**(0.01, 0.18)**	-0.04	(-0.80, 0.49)
Plant size	**0.79**	**(0.47, 1.09)**	**1.26**	**(1.09, 1.43)**	**3.78**	**(3.04, 4.61)**	**0.58**	**(0.49, 0.69)**	-	-
(Plant size)^2	**-0.56**	**(-0.88, -0.3)**	**-0.71**	**(-0.87, -0.57)**	**-1.37**	**(-2.21, -0.74)**	**-0.26**	**(-0.37, -0.18)**	-	-
T_{mean}	-3.52	(-5.08, 0.22)	0.35	(-0.24, 1.75)	0.04	(-2.34, 2.53)	-0.06	(-0.58, 0.41)	0.55	(-2.47, 3.33)
$(T_{mean})^2$	**3.37**	**(0.17, 5.04)**	-0.51	(-1.76, 0.16)	-0.13	(-2.66, 2.24)	-0.02	(-0.42, 0.52)	0.52	(-2.67, 3.20)
T_{range}	-0.40	(-0.95, 0.05)	0.01	(-0.23, 0.25)	0.33	(-0.10, 1.19)	0.11	(0.00, 0.20)	**-0.63**	**(-1.78, -0.07)**
Random effects										
Site (Intercept)	0.00	(0.00, 0.55)	0.08	(0.00, 0.55)	0.00	(0.00, 0.72)	0.12	(0.00, 0.23)	0.00	(0.00, 0.40)
Year (Intercept)	0.51	(0.22, 0.86)	0.41	(0.33, 0.50)	1.09	(0.84, 1.40)	0.15	(0.11, 0.19)	0.00	(0.00, 0.70)
Year ($SoilVeg_2$)	1.27	(0.82, 1.83)	-	-	-	-	-	-	-	-
Year (Intercept * $SoilVeg_2$)	0.15	(-0.48, 0.98)	-	-	-	-	-	-	-	-
Plot (Intercept)	-	-	-	-	1.28	(0.87, 1.88)	-	-	-	-
Plot (Plant size)	-	-	-	-	1.52	(0.85, 2.56)	-	-	-	-
Plot (Intercept * Plant size)	-	-	-	-	0.95	(0.74, 1.00)	-	-	-	-
Residual	-	-	1.62	(1.39, 1.89)	-	-	0.36	(0.34, 0.38)	2.61	(0.86, 13436)
Marginal R^2	0.07	(0.03, 0.12)	0.25	(0.2, 0.31)	0.46	(0.38, 0.56)	0.44	(0.36, 0.53)	0.04	(0.00, 0.10)
Conditional R^2	0.41	(0.29, 0.56)	0.36	(0.3, 0.49)	0.80	(0.69, 0.88)	0.57	(0.51, 0.64)	0.05	(0.02, 0.18)

For each of the five vital rates, the table reports the standardized coefficients of fixed effect, the standard deviation of random effects (intercepts and slopes), the correlations between random intercept and slopes and marginal and conditional R^2 (Nakagawa *et al.* 2017). Only the random effects that were retained after model selection on the random structure are shown. Means and 95% confidence intervals were calculated by randomly sampling statistical models over 200 bootstrapped demographic datasets and 10 resampled imputed datasets. The predictors whose confidence intervals do not overlap with zero are in **bold**.